This article was downloaded by: [University Of Gujrat]
On: 11 December 2014, At: 13:59
Publisher: Taylor & Francis
Informa Ltd Registered in England and Wales Registered Number: 1072954 Registered office: Mortimer House, 37-41 Mortimer Street, London W1T 3JH, UK

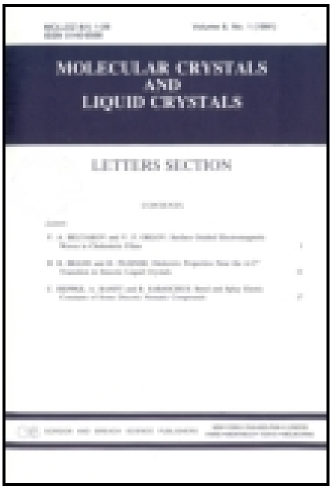

Molecular Crystals and Liquid Crystals
Publication details, including instructions for authors and subscription information:
http://www.tandfonline.com/loi/gmcl20

Efficiency Improvement of Dye-Sensitized Solar Cells Using WO_3

Tae Sung Eom[a], Kyung Hwan Kim[a], Chung Wung Bark[a] & Hyung Wook Choi[a]
[a] Department of Electrical Engineering, Gachon University, Sujeong-Gu, Seongnam-Si, Gyeonggi-Do, Korea

Published online: 06 Dec 2014.

To cite this article: Tae Sung Eom, Kyung Hwan Kim, Chung Wung Bark & Hyung Wook Choi (2014) Efficiency Improvement of Dye-Sensitized Solar Cells Using WO_3, Molecular Crystals and Liquid Crystals, 602:1, 81-87, DOI: 10.1080/15421406.2014.944675

To link to this article: http://dx.doi.org/10.1080/15421406.2014.944675

PLEASE SCROLL DOWN FOR ARTICLE

Taylor & Francis makes every effort to ensure the accuracy of all the information (the "Content") contained in the publications on our platform. However, Taylor & Francis, our agents, and our licensors make no representations or warranties whatsoever as to the accuracy, completeness, or suitability for any purpose of the Content. Any opinions and views expressed in this publication are the opinions and views of the authors, and are not the views of or endorsed by Taylor & Francis. The accuracy of the Content should not be relied upon and should be independently verified with primary sources of information. Taylor and Francis shall not be liable for any losses, actions, claims, proceedings, demands, costs, expenses, damages, and other liabilities whatsoever or howsoever caused arising directly or indirectly in connection with, in relation to or arising out of the use of the Content.

This article may be used for research, teaching, and private study purposes. Any substantial or systematic reproduction, redistribution, reselling, loan, sub-licensing, systematic supply, or distribution in any form to anyone is expressly forbidden. Terms & Conditions of access and use can be found at http://www.tandfonline.com/page/terms-and-conditions

Mol. Cryst. Liq. Cryst., Vol. 602: pp. 81–87, 2014
Copyright © Taylor & Francis Group, LLC
ISSN: 1542-1406 print/1563-5287 online
DOI: 10.1080/15421406.2014.944675

Efficiency Improvement of Dye-Sensitized Solar Cells Using WO_3

TAE SUNG EOM, KYUNG HWAN KIM,
CHUNG WUNG BARK, AND HYUNG WOOK CHOI*

Department of Electrical Engineering, Gachon University, Sujeong-Gu,
Seongnam-Si, Gyeonggi-Do, Korea

In this work, we report for the first time the improvement of the photovoltaic characteristics of DSSCs by mixing TiO_2 with WO_3. WO_3 reduced the surface trap states of TiO_2, which suppressed the charge recombination and increased the driving force of electron injection, thereby improving its power conversion efficiency. It was observed that DSSCs fabricated using the WO_3-mixed TiO_2 films show the maximum conversion efficiency of 4.84% because of the effective prevention of the electron recombination. DSSCs based on WO_3-mixed TiO_2 films showed better photovoltaic performance than cells fabricated with only TiO_2 nanoparticles.

Keywords DSSCs; WO_3; TiO_2; mixture; photovoltaic performance; electron recombination

Introduction

Dye-sensitized solar cells (DSSCs) have been intensively studied since their discovery in 1991 [1]. They are attracting considerable interest for use in next-generation energy-harvesting devices because of their simple structure and process, low-cost fabrication, transparency, color control, and applicability in flexible DSSCs [2–4]. A DSSC is composed of a dye-adsorbed nanoporous TiO_2 layer on a fluorine-doped tin oxide (FTO) glass substrate, redox electrolytes, and a counter electrode. The heart of the system is a mesoporous TiO_2 film composed of nanometer-sized particles possessing a large specific surface area. However, an unusual feature of such DSSCs is the lack of a space charge layer, which separates the injected electrons from the holes in the dye or electrolyte [5–8]. A unidirectional charge flow with no electron leakage at the interfaces is essential for high energy-conversion efficiency [9]. It has been reported that the efficiency of DSSCs can be improved by the surface modification of TiO_2 with insulating oxides or high-band-gap semiconductors to form a blocking layer that prevents charge recombination at the TiO_2/dye/electrolyte interface [10–13].

In this paper, we investigate the effect of WO_3-mixed TiO_2 films on DSSCs. DSSCs were fabricated by mixing various percentages of WO_3 and TiO_2 nanoparticle composite

---

*Address correspondence to Prof. Hyung Wook Choi, Department of Electrical Engineering, Gachon University, 1342 SeongnamDaero, Sujeong-gu, SeongNam, Gyeonggi-do, 461-701, Korea (ROK). E-mail: chw@gachon.ac.kr

Color versions of one or more of the figures in the article can be found online at www.tandfonline.com/gmcl.

particles. The TiO_2 layer was coated on the FTO glass by the doctor blade method. A dye of ruthenium(II) (N-719) and an electrolyte (I^-/I_3^-) were used in the fabrication process. The impedance results indicate improved electron transport at the TiO_2/dye/electrolyte interface. As a result, DSSCs based on WO_3-mixed TiO_2 films showed better photovoltaic performance than those made of only TiO_2 nanoparticles.

Experimental

Tetra titanium isopropoxide (TTIP, Aldrich Chemical), ethyl alcohol, nitric acid, and DI water were used as the starting materials. The TiO_2 powders were manufactured by a sol-gel method and TiO_2 pastes were prepared as per references [14, 15]. Nanoporous TiO_2 upper layers were coated on the passivating layer-coated FTO glass using the doctor blade method. The prepared TiO_2 electrode was sintered at 450°C for 15 min and at 500°C for 15 min in air.

WO_3-mixed TiO_2 films were prepared using various stoichiometric ratios of tungstate oxide (WO_3 nanopowder, 100 nm, Aldrich) to obtain a weight percentage of WO_3 to TiO_2 ranging from 1 wt% to 100 wt%.

The nanoporous TiO_2 electrode films were immersed in an N719 dye complex for 24 h at room temperature. A counter-electrode was prepared by spin-coating a H_2PtCl_6 solution onto the FTO glass and heating it at 450°C for 30 min. The dye-adsorbed TiO_2 electrode and the Pt counter-electrode were assembled onto a sandwich-type cell and sealed with a 60-μm-thick hot-melt sealant. An electrolyte solution was introduced through a drilled hole in the counter-electrode. The hole was then sealed using a cover glass.

The morphology and the thickness of the prepared passivating layers were investigated using field-emission scanning electron microscopy (FE-SEM, S-4700, Hitachi). The conversion efficiency and electrochemical impedance spectroscopy (EIS) of the fabricated DSSCs were measured using an I–V solar simulator (Solar Simulator, McScience). The active area of the resulting cell exposed to light was approximately 0.25 cm^2 (0.5 cm × 0.5 cm). The absorbance of the TiO_2 thin films was measured using a UV spectrometer (UV-Vis 8453, Agilent).

Results and Discussion

Figure 1(a) shows the XRD pattern of the tungsten oxide. Figure 1(b) shows that the XRD pattern of the TiO_2 powders at 500°C are a mixture of anatase and rutile phases. In the WO_3 phase, the XRD pattern [Fig. 1(c)]. shows that the WO_3-mixed TiO_2 surface is sufficient to crystallize the form (W1-W3). The XRD pattern of WO_3 shows prominent WO3 peaks, denoted as W1 (002), W2 (020), and W3 (220), which were measured with JCPDS(43-1035).

Figure 2(a) shows that the diameters of the TiO_2 nanoparticles prepared by the sol-gel method lie within 20–30 nm. Figure 2(b) shows the mixture of TiO_2 and WO_3 surfaces. Figure 2(c) shows that the diameters of the WO_3 nanoparticles prepared by the sol-gel method also lie within 90–110 nm. The SEM results show that the grain size of the WO_3 nanoparticles is larger than that of the TiO_2 nanoparticles.

Figure 3 shows the EIS of WO_3 at various stoichiometric ratios. The EIS analysis is used to investigate the electron-transport and recombination in DSSCs. The small semicircle is fitted to a charge-transfer resistance (R1) and a constant phase, and the large semicircle is fitted to a transfer resistance (R2) and a constant phase. Because R1 is not affected by WO_3,

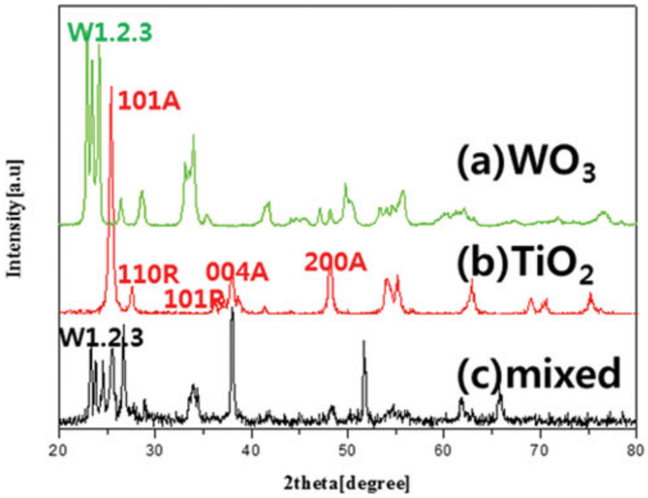

Figure 1. The XRD patterns of the WO_3-mixed films. (a) WO_3, (b) TiO_2, (c) WO_3-mixed TiO_2 films.

we can focus chiefly on R2. The first semicircle is a minimum for 5 wt% WO_3, which is related to the charge-transfer resistances of the FTO/TiO_2 and TiO_2/electrolyte interfaces (R2). The decrease in R2 for 5 wt% WO_3 indicates a reduction in electron recombination and greater efficiency of electron transport. However, in the case of 10 wt% WO_3, R2 is

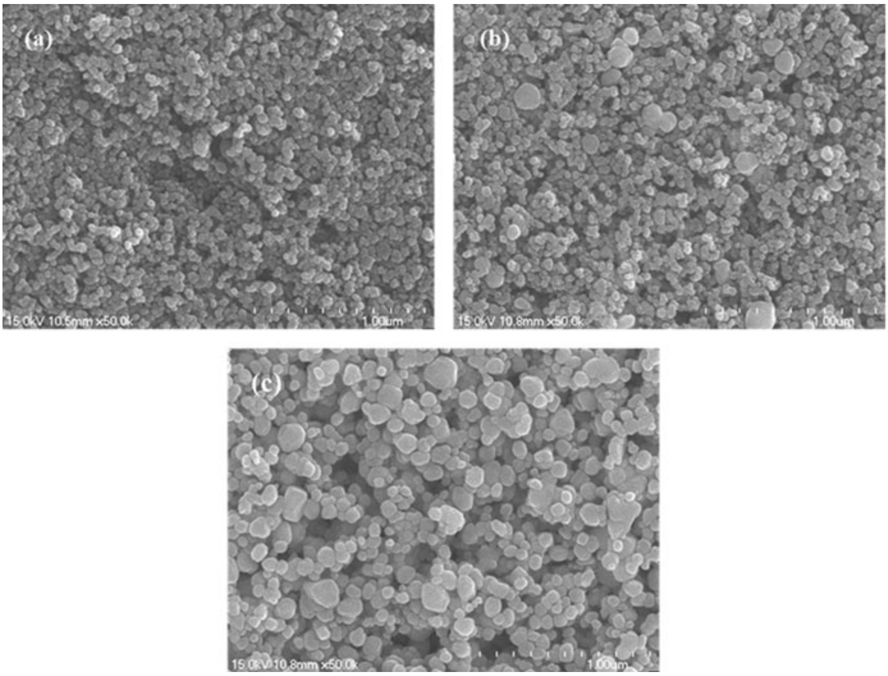

Figure 2. Surface FE-SEM images (a) TiO_2 films (b) WO_3-mixed TiO_2 films, (c) WO_3 films.

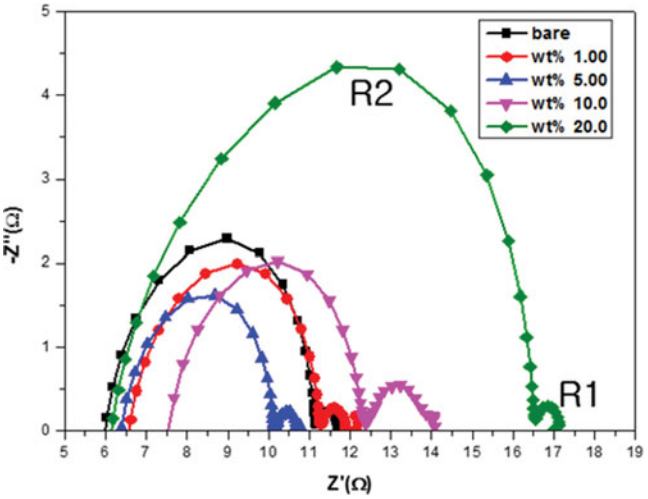

Figure 3. Electrochemical impedance spectra of the WO_3-mixed TiO_2 films.

increased because 10 wt% WO_3, which has more trap sites, obstructs the movement of electrons from the nanoporous TiO_2 layer to the FTO electrode.

Figure 4 shows how the UV-vis absorbance of the WO_3-mixed TiO_2 films affects the dye absorption. It is known that N-719 dye shows absorption peaks. Figure 4 shows the absorption spectrum of N-719 dye in the 400–800 nm wavelength range in TiO_2 electrode films with different composition (1–20 wt% WO_3). At wavelengths 400–500 nm, the absorbance of the sample containing 5 wt% WO_3 is the highest and the absorbance of the sample containing 20 wt% WO_3 is the lowest. It is thought that a nanoparticle with the different sizes in a photoelectric can scatter the incident light of different wavelengths in the range of visible light [16, 17]. Therefore, the TiO_2 layer with the dye serves as a photoactive layer.

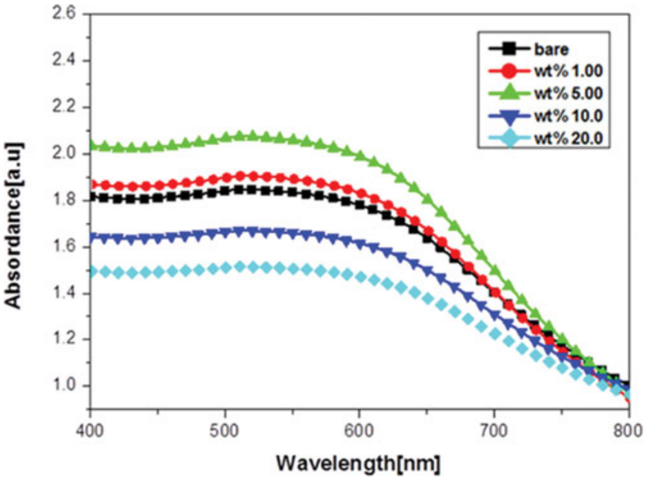

Figure 4. UV-vis absorption spectra of the WO_3-mixed TiO_2 films.

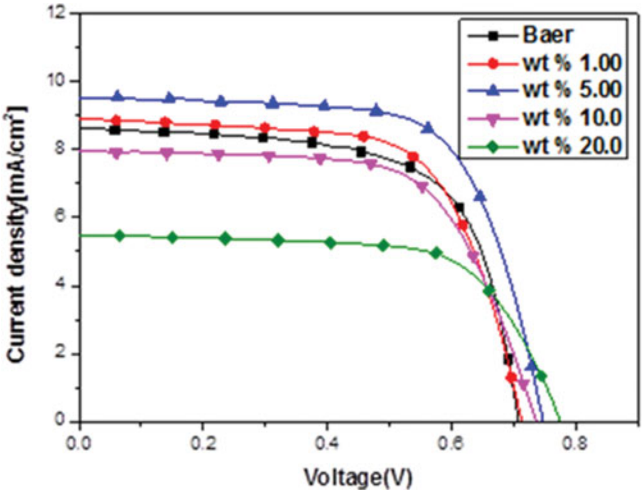

Figure 5. I–V characteristics of WO_3-mixed TiO_2 films.

Extending the retention period of light in a DSSC by creating a light scattering layer in the working electrode is one of promising approaches to enhance the performance of a DSSC.

Figure 5 shows the I–V characteristics of the TiO_2 layers for different mixtures of WO_3. The corresponding photovoltaic parameters of DSSCs are summarized in Table 1. The internal resistance decreases as a function of the WO_3 mixture, which confirmed the previous discussion about the blocking effect of WO_3 on charge recombination shown in Fig. 3. A mechanism for preventing this voltage drop is shown in Fig. 6. The electrons that would flow to the dye or the electrolyte can be confined in the conduction band (CB) of WO_3; these confined electrons travel through the CB of WO_3. The downward shift of the conduction band increased the driving force of the photo generated electrons transfer from the excited dye to the conduction band of the TiO_2, thus improving the electron injection efficiency [18–20]. It can be seen from Table 1 that the amount of WO_3 has different effects on the open-circuit voltage (Voc), short-circuit current (Jsc), and overall conversion efficiency (η). The Voc value of DSSCs increased as a function of the WO_3 mixture. One of the most important parameters for a solar cell is its photoelectric conversion efficiency. DSSCs fabricated using 5 wt% WO_3 exhibited higher conversion efficiency, with

Table 1. Jsc, Voc, FF, and efficiency

Sample	Jsc (mA/cm^2)	Voc (V)	FF (%)	η (%)
Bare	8.63	0.70	66.04	4.03
wt.% 1.00	8.90	0.71	65.95	4.19
wt.% 5.00	9.52	0.74	68.09	4.84
wt.% 10.0	7.95	0.73	65.26	3.82
wt.% 20.0	5.47	0.77	67.23	2.85
wt.% 30.0	4.21	0.77	65.12	2.13
wt.% 50.0	5.20	0.72	57.69	2.17
wt.% 100	1.67	0.72	43.73	0.53

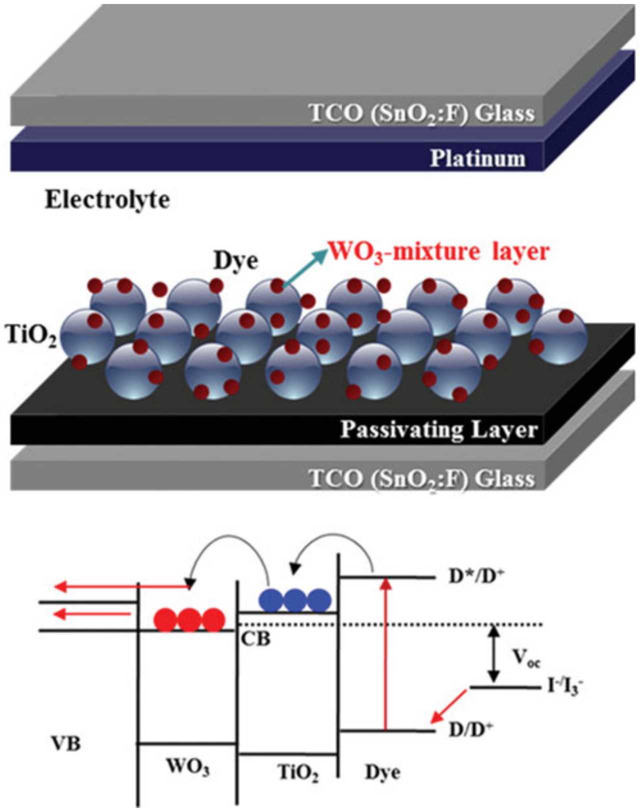

Figure 6. (a) Schematic diagram of the flexible DSSC of WO_3-mixed TiO_2 films and (b) suggested mechanism to improve the efficiency of the DSSCs that were prepared by using the WO_3-mixed cells.

a photocurrent density (Jsc) of 9.52 mA/cm^2, Voc of 0.74 V, and cell conversion efficiency of 4.84%. DSSCs have higher Voc as compared to that of the bare cell; their Jsc was also higher. The dependence of WO_3 mixture on the overall conversion efficiency showed the same trend as with the short-circuit photocurrent. However, higher concentrations of WO_3 (1–100 wt%) reduced the solar cell performance.

Conclusions

In this work, we report for the first time the improvement in the photovoltaic characteristics of DSSCs by mixing TiO_2 with WO_3. DSSCs were fabricated using WO_3 of various percentages mixed with TiO_2 nanoparticle composite particles. The DSSC prepared without WO_3 had a Jsc of 8.63 A/cm^2, Voc of 0.70 V, and η of 4.03%. The DSSC using 5 wt% WO_3 had the maximum conversion efficiency of 4.84% because of the effective electron transport. In addition, the DSSC composite cell fabricated using 5 wt% WO_3 showed better photovoltaic performance than the TiO_2 nanoparticle cell without WO_3. It was observed that with increased efficiency, internal resistance decreased. Thus, the use of WO_3-mixed TiO_2 films was demonstrated to be an effective method to improve the efficiency of TiO_2 nanoparticle-based DSSCs.

Funding

This work was supported by the Human Resources Development program (No. 20124030200010) of the Korea Institute of Energy Technology Evaluation and Planning (KETEP) grant funded by the Korea government Ministry of Trade, Industry and Energy. This work was supported by the National Research Foundation of Korea (NRF) Grant Funded by the Korean Government (MEST) (No. 2012R1A1A2044472).

References

[1] O'Regan, B., & Grätzel, M. (1991). *Nature*, *353*, 737–740.

[2] Grätzel, M. (2003). *J. Photochem. Photobiol. C. Rev.*, *4*, 145–153.

[3] Nogueria, A. F., Longo, C., & De Paoli, M.-A. (2004). *Coord. Chem. Rev.*, *248*, 1455–1468.

[4] Gregg, B. A. (2004). *Coord. Chem. Rev.*, *248*, 1215–1224.

[5] Chappel, S., Chen, S. G., & Zaban, A. (2002). *Langmuir*, *18*, 3336.

[6] Cahen, D., Hodes, G., Gratzel, M., Guillemoles, J. F., & Riess, I. (2000). *J. Phys. Chem. B*, *104*, 2053.

[7] Ni, M., Leung, M. K. H., Leung, D. Y. C., & Sumathy, K. (2006). *Sol. Energy Mater. Sol. Cells*, *90*, 1331.

[8] Chou, C. S., Yang, R. Y., Yeh, C. K., & Lin, Y. J. (2009). *Powder Technol.*, *194*, 95.

[9] Xia, J., Masaki, N., Jiang, K., Wada, Y., & Yanagida, S. (2006). *Chem. Lett.*, 35.

[10] Alarcon, H., Boschloo, G., Mendoza, P., Solis, J. L., & Hagfeldt, A. (2005). *J. Phys. Chem. B*, *109*, 18483.

[11] Chen, S. G., Chappel, S., Diamant, Y., & Zaban, A. (2001). *Chem. Mater.*, *13*, 4629.

[12] Wang, Z.-S., Huang, C.-H., Huang, Y.-Y., Hou, Y.-J., Xie, P.-H., Zhang, B.-W., & Cheng, H.-M. (2001) *Chem. Mater.*, *13*, 678.

[13] Jung, H. S., Lee, J. K., Nastasi, M., Lee, S. W., Kim, J. Y., Park, J. S., Hong, K. S., & Shin, H. (2005). *Langmuir*, *21*, 10332.

[14] Jin, Y. S., Kim, K. H., Park, S. J., Kim, J. H., & Choi, H. W. (2010). *J. Korean Phys. Soc.*, *57*, 1049–1053.

[15] Jin, Y. S., Kim, K. H., Park, S. J., Yoon, H. H., & Choi, H. W. (2011). *J. Nanosci. Nanotechnology 11*, 10971–10975.

[16] Ferber, J., & Luther, J. (1998). *Sol. Energy Mater. Sol. Cells*, *54*, 265.

[17] Kim, S.-H., Cho, Y.-S., Jeon, S.-J., Eun, T. H., Yi, G.-R., & Yang, S.-M. (2008). *Adv. Mater.*, *20*, 3268.

[18] Boschloo, G., Lindstrom, H., Magnusson, E., Holmberg, A., & Hagfeldt, A. (2002). *J. Photochem. Photobiol. A: Chem.*, *148*, 11.

[19] Haque, S. A., Palomares, E., Cho, B. M., Green, A. N. M., Hirata, N., Klug, D. R., & Durrant, J. R. (2005). *J. Am. Chem. Soc.*, *127*, 3456.

[20] Cheng, P., Deng, C., Dai, X., Li, B., Liu, D., & Xu, J. (2008). *J. Photochemistry and Photobiology A: Chemistry*. *195*, 144–150.